INSTITUTE OF PHYSICS PUBLISHING PHYSIOLOGICAL MEASUREMENT

Physiol. Meas. **26** (2005) 885–901 doi:10.1088/0967-3334/26/6/001

Effects of the time response of the temperature sensor on thermodilution measurements

Adson F da Rocha[1], Icaro dos Santos[1], Francisco A O Nascimento[1], Maxwell D B Melo[1], Dieter Haemmerich[2] and Jonathan W Valvano[3]

[1] Department of Electrical Engineering, University of Brasilia, Brasilia, DF 70910-900, Brazil
[2] Division of Pediatric Cardiology, Medical University of South Carolina, Charleston, SC 29425, USA
[3] Department of Electrical and Computer Engineering, The University of Texas at Austin, Austin, TX 78712, USA

E-mail: haemmer@musc.edu

Received 12 April 2005, accepted for publication 29 July 2005
Published 23 September 2005
Online at stacks.iop.org/PM/26/885

Abstract

Thermodilution is widely used to measure cardiac output, ejection fraction and end diastolic volume. Even though the method is based on dynamic temperature measurements, little attention has been paid to the characterization of the dynamic behavior of the temperature sensor and to its influence on the accuracy of the method. This paper presents several theoretical and empirical results related to the thermodilution method. The results show that, at flow velocities above 0.2 m s^{-1}, the response of temperature sensors embedded in Swan–Ganz catheters can be accurately described by a convolution operation between the true temperature of the blood and the impulse response of the sensor. The model developed is used to assess the influence of the probe response on the measurement of cardiac output, and this study leads us to the conclusion that the probe response can cause errors in the cardiac output measurement, but this error is usually small (2% in cases with a high degree of arrhythmia). The results show that these small errors appear during arrhythmias that affect the R–R interval and when the real temperature distribution at the pulmonary artery does not possess a shape with perfect temperature plateaux.

Keywords: thermodilution, thermistor, cardiac output, Swan–Ganz

1. Introduction

For several decades, the thermodilution method has been used in intensive care units for monitoring cardiac output (Webster 1988). This technique, initially proposed by

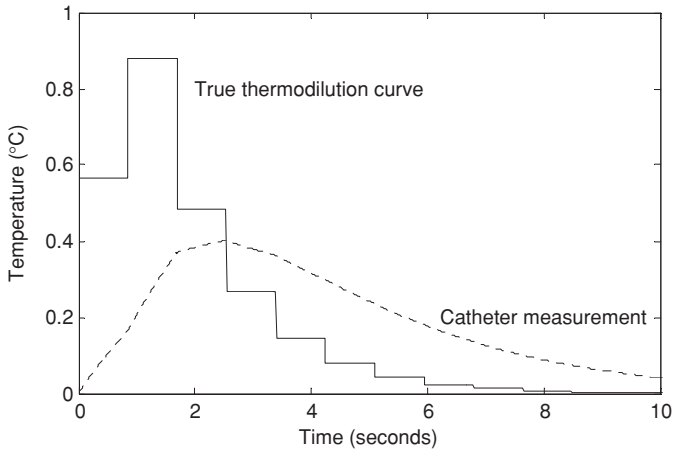

Figure 1. An idealization of the thermodilution curve (solid line) and the corresponding curve that would be measured by a temperature sensor with slow time response (dotted line).

Fegler (1954, 1957), is a variation of the so-called Stewart–Hamilton method (Trautman and Newbower 1984, 1988). Fegler's method consisted of rapidly injecting a small amount of cold Ringer's solution into the vena cava and recording the temperature in the pulmonary artery and in the right ventricle. Thus, Fegler's method has the advantage that the indicator is a harmless entity (heat), which is easily absorbed by the body. Swan and Ganz (Swan *et al* 1970, Ganz and Swan 1972) popularized the use of a pulmonary artery pressure catheter with an injection port and an embedded thermistor for the measurement of cardiac output, and these catheters are commonly called Swan–Ganz catheters. The indicator and thermodilution methods are extensively described in the literature (Bloomfield 1973, Trautman and Newbower 1984, 1988, Dow 1956, Taylor and Sheffer 1990, von Reith and Versprille 1988, Webster 1998).

Despite the large number of references available on thermodilution methods, there are very few studies (Marushak and Schauble 1985) on the temperature sensor dynamics and on its influence on the thermodilution-based measurements. In this study, we address these issues.

The solid line in figure 1 shows an idealization of the time course of temperature in the pulmonary artery after the sudden injection of a bolus of a liquid at a temperature that is higher than the blood temperature. Note that we chose to plot the temperature as a positive curve, starting from 0 °C instead of the baseline blood temperature. Thermodilution curves are usually plotted using this normalization.

In the actual temperature profile measured by the temperature sensor, the plateaux are not perfectly flat and the transitions are not perfect steps. This is due to imperfect mixing in the cardiovascular system. The actual measured curve looks like the dotted line curve in figure 1. The measurement is a smeared version of the actual temperature. This effect is due to the insulation and the thermal mass of the temperature sensor, resulting in thermal inertia and smearing of the measured signal.

The cardiac output is approximately inversely proportional to the area under the true thermodilution curve, shown as a solid line in figure 1 (Rocha 1997). However, from our catheter we obtain a curve deviating from the true thermodilution curve (dotted line in figure 1), which is used to calculate the area under the curve.

It is conceivable that the smoothing of the temperature time course by the temperature sensor leads to errors in the thermodilution method. However, usually it is assumed that the

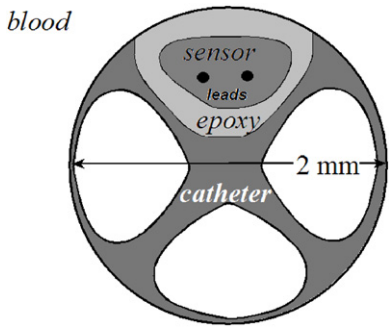

Figure 2. A model for a thermistor probe: an approximated cross-section of the Swan–Ganz catheter.

area under the curve is preserved regardless of the probe response. In this study, we provide strong theoretical evidence that this is only approximately true. We also provide a theoretical model for the behavior of thermistor probes, and we report a series of experiments which confirm the validity of this model. We show that, under certain conditions, the Swan–Ganz thermistor behaves like a linear time-invariant low-pass filter, and we explore the consequences of this finding.

These findings are important because they provide strong theoretical support for some assumptions based on empirical knowledge that usually are made in the thermodilution method. These assumptions have consequences in the bolus injection method used for cardiac output, as well as in the modern catheters that allow continuous monitoring of cardiac output, ejection fraction and end diastolic volume.

2. Theoretical model for the temperature sensor

2.1. Theoretical model

A general method for modeling the response of temperature sensors was proposed by Rocha (1997). Even though this method has general applicability and can be applied to any temperature sensor surrounded by a medium with constant convection coefficient, it will be used here to model the thermistor probe embedded in a Swan–Ganz catheter. A model of the probe is illustrated in figure 2.

The probe is assumed to be in a convective field, and it will be assumed that the convection coefficient is constant in time, even though it can be non-uniform along the boundary. The requirement of a constant, non-uniform convection coefficient will make it possible to write a linear time-invariant relationship between the true and measured temperatures. The bulk temperature of the fluid will be the magnitude to be measured.

The approach we use is, to first find the step response of the sensor, and then use Duhamel's superposition theorem to find a general convolutional relationship (Rocha 1997).

The method proposed by Rocha (1997) can be used to find the time response of probes with complex geometries. In most of the cases, the probe behavior does not have a strict 1D characteristic. However, in many cases, a 1D model can be effectively used as an approximation. This section presents a simplified model for a thermistor embedded in a thermodilution catheter. The thermistor is located a few centimeters from the catheter tip of the Swan–Ganz, and it is protected by an epoxy cap, as illustrated in figure 2.

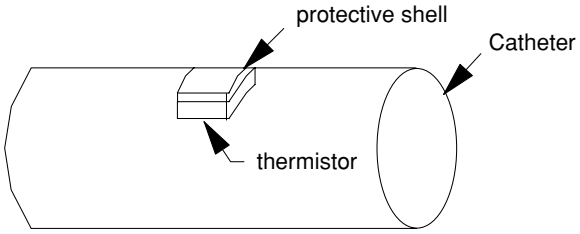

Figure 3. A simplified model for the thermistor probe.

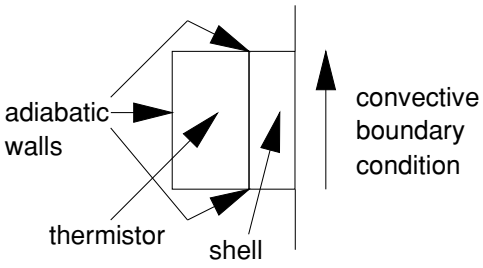

Figure 4. A model for the thermistor: the catheter walls are considered to be adiabatic.

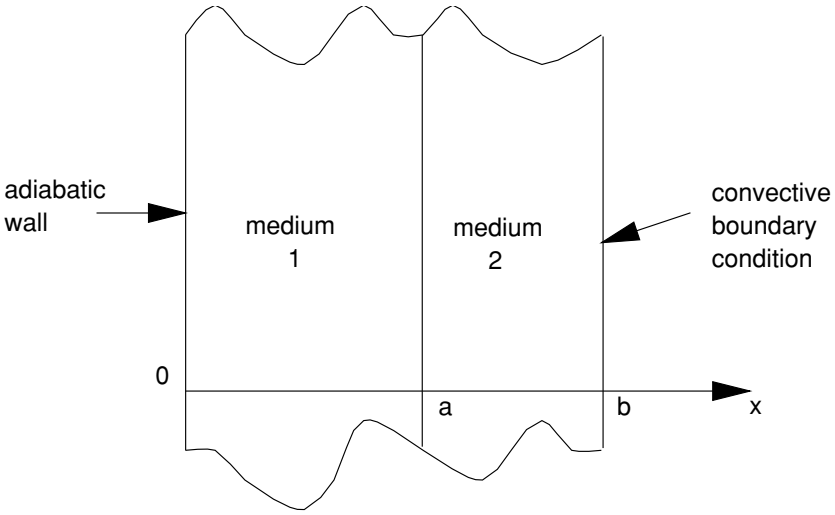

Figure 5. A 1D approximated model.

Figure 3 shows a model for the thermistor probe in the catheter. Some simplifications are adopted. In the real catheter, the thermistor would not have the shape of a parallelepiped (i.e. box with angles different from 90°), but the shape of an oblate spheroid. Also, the coating would not have a uniform thickness. However, the model will provide an excellent qualitative and quantitative understanding of the behavior of the probe.

Another simplifying assumption will be that the catheter body is adiabatic, resulting in further simplification of the model, as shown in figure 4.

Since the lateral walls are considered to be adiabatic, the model above is equivalent to a 1D problem, as illustrated in figure 5.

The problem was solved using the orthogonal expansion technique (Mikhailov and Ozisik 1984).

The following variables are defined:

$T_1(x,t)$ = temperature of the thermistor core;
$T_2(x,t)$ = temperature of the shell.

To calculate the step response of the sensor, the initial temperature in the probe is assumed to be constant ($=V$) in the thermistor body and in the shell, and the bulk temperature of the fluid is zero. The usual definition of a step response is the response to bulk temperature changing from 0 to 1. We chose to use a step with initial temperature V and end temperature 0 as perturbation because this choice results in a homogeneous problem without the need for a change of variables.

The heat-transfer equations for media 1 (thermistor) and 2 (shell) are

$$\frac{\partial^2 T_1(x,t)}{\partial x^2} = \frac{1}{\alpha_1}\frac{\partial T_1(x,t)}{\partial t} \qquad \text{for} \quad 0 \leqslant x < a, \tag{1}$$

$$\frac{\partial^2 T_2(x,t)}{\partial x^2} = \frac{1}{\alpha_2}\frac{\partial T_2(x,t)}{\partial t} \qquad \text{for} \quad a < x < b. \tag{2}$$

The initial conditions are

$$T_1(x,0) = F_1(x) \qquad \text{for} \quad 0 < x < a, \tag{3}$$

$$T_2(x,0) = F_2(x) \qquad \text{for} \quad a < x < b. \tag{4}$$

The boundary conditions are

$$\left.\frac{\partial T_1}{\mathrm{d}x}(x,t)\right|_{x=0} = 0, \tag{5}$$

$$T_1(a,t) = T_2(a,t) \qquad \text{for} \quad t > 0, \tag{6}$$

$$k_1 \left.\frac{\partial T_1(x,t)}{\partial x}\right|_{x=a} = k_2 \left.\frac{\partial T_2(x,t)}{\partial x}\right|_{x=a}, \tag{7}$$

$$k_2^* \frac{\partial T_2(x,t)}{\partial x} + h_3^* T_2(x,t) = 0. \tag{8}$$

The asterisks in k_2^* and h_3^* are used to indicate that they can be used as parameters, and conditions of the first and second kind are obtainable from the general result. In order to obtain a more general result, the initial conditions were assumed to be equal to $F_1(x)$ and $F_2(x)$. Later, these values are replaced by V.

Assuming a solution of the form

$$T(x,t) = \psi(x)\Gamma(t), \tag{9}$$

the solutions for the regions $0 < x < a$ and $a < x < b$ (Rocha 1997) are

$$T_1(x,t) = \sum_{n=1}^{\infty} \frac{1}{N_n} \mathrm{e}^{-\beta_n^2 t} \Psi_{1,n}(x) \left[\frac{k_1}{\alpha_1} \int_{x'=0}^{a} \Psi_{1,n}(x') F_1(x')\,\mathrm{d}x' + \frac{k_2}{\alpha_2} \int_a^b \Psi_{2,n}(x') F_2(x')\,\mathrm{d}x' \right], \tag{10}$$

$$T_2(x,t) = \sum_{n=1}^{\infty} \frac{1}{N_n} \mathrm{e}^{-\beta_n^2} \Psi_{2,n}(x) \left[\frac{k_1}{\alpha_1} \int_{x'=0}^{a} \Psi_{1,n}(x') F_1(x')\,\mathrm{d}x' + \frac{k_2}{\alpha_2} \int_a^b \Psi_{2,n}(x') F_2(x')\,\mathrm{d}x' \right], \tag{11}$$

where

$$N_n = \frac{k_1}{\alpha_1}\int_0^a \Psi_{1,n}^2(x')\,\mathrm{d}x' + \frac{k_2}{\alpha_2}\int_a^b \Psi_{2,n}^2(x')\,\mathrm{d}x' \tag{12}$$

and

$$\psi_1(r) = \cos\left(\frac{\beta_n}{\sqrt{\alpha_1}}x\right), \tag{13}$$

$$\psi_2(r) = A_{2,n}\sin\left(\frac{\beta_n}{\sqrt{\alpha_2}}x\right) + B_{2,n}\cos\left(\frac{\beta_n}{\sqrt{\alpha_2}}x\right), \tag{14}$$

$$A_{2,n} = \cos(\gamma)\sin\left(\frac{a}{b}\eta\right) - K\sin(\gamma)\cos\left(\frac{a}{b}\eta\right), \tag{15}$$

$$B_{2,n} = K\sin(\gamma)\sin\left(\frac{a}{b}\eta\right) + \cos(\gamma)\cos\left(\frac{a}{b}\eta\right), \tag{16}$$

$$K = \frac{k_1}{k_2}\sqrt{\frac{\alpha_2}{\alpha_1}}, \tag{17}$$

$$\gamma = \frac{a\beta_n}{\sqrt{\alpha_1}}, \tag{18}$$

$$\eta = \frac{b\beta_n}{\sqrt{\alpha_2}}, \tag{19}$$

$$H = \frac{bh_3^*}{k_2^*}. \tag{20}$$

The eigenvalues β_n are the values for which the following determinant is zero:

$$\begin{vmatrix} \cos(\gamma) & -\sin\left(\frac{a}{b}\eta\right) & -\cos\left(\frac{a}{b}\eta\right) \\ -K\sin(\gamma) & -\cos\left(\frac{a}{b}\eta\right) & \sin\left(\frac{a}{b}\eta\right) \\ 0 & \frac{H}{\eta}\sin(\eta) + \cos(\eta) & \frac{H}{\eta}\cos(\eta) - \sin(\eta) \end{vmatrix} = 0. \tag{21}$$

The measured temperature is assumed to be the volumetric average of $T_1(x,t)$, in equation (10), but we will show later on that even if the measured temperature is a weighted average of the temperature distribution in the core, the weighting function of the electrical conversion is not important for cardiac output measurements. By performing this volumetric average of the temperature distribution in the thermistor core, one can show that the probe response in a convective medium can always be expressed as a summation of exponential components, as shown in equation (22):

$$T_{\mathrm{meas}}(t) = \sum_{n=1}^{\infty} d_n\,\mathrm{e}^{-\lambda_n^2 t}. \tag{22}$$

The next step for characterizing the sensor response is to use Duhamel's equation (Ozisik 1993) to write the convolutional response to a generic input $T_\infty(t)$, as shown in equation (23):

$$T_{\mathrm{gen,meas}}(t) = \int_{\tau=0}^{t} T_\infty(\tau)\frac{\partial T_{\mathrm{step}}(t-\tau)}{\partial t}\,\mathrm{d}\tau. \tag{23}$$

The term T_{step} corresponds to the step response of the sensor ($T_{\mathrm{step}}(t) = 1 - T_{\mathrm{meas}}(t)$), with $V = 1$. Thus, equation (23) shows that the sensor behaves as a linear time-invariant

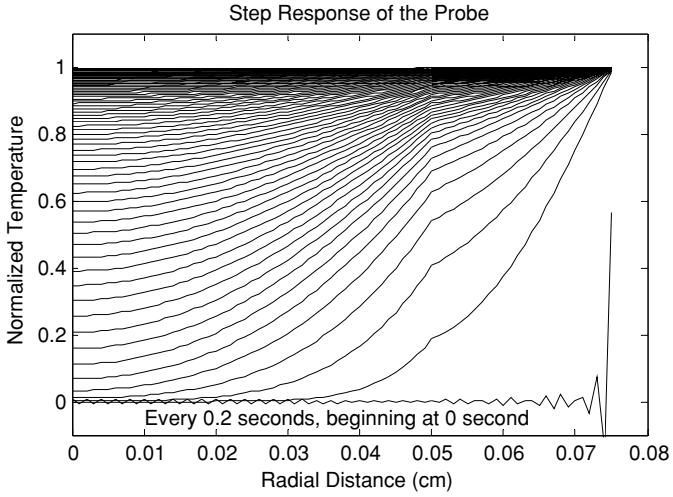

Figure 6. Step response of the thermistor sensor when the convection coefficient is 10 W cm^{-2} K^{-1}. The normalized temperature goes from 0 to 1 outside the probe at $t = 0$ s. The lowest curve is the temperature at 0 s, and time increases by 0.2 s with each successive curve. The probe center is positioned at $x = 0$, the boundary of the thermistor core is at $x = 0.05$ and the shell boundary is at $x = 0.08$.

operator, and that the measured temperature is equal to a convolution of the real temperature with the impulse response of the probe.

The equations above can be used to analyze the nature of the catheter response. To do this, we will assume typical thermal properties for the thermistor, for the shell and for the convection coefficient. These values were based on rough estimates and are for qualitative analysis. The adopted values are $a = 0.05$ cm, $b = 0.075$ cm, $k_1 = 0.001$ W cm^{-1} °C^{-1}, $k_2^* = 0.003$ W cm^{-1} °C^{-1}, $\alpha_1 = 0.001$ cm^2 s^{-1}, $\alpha_2 = 0.0014$ cm^2 s^{-1}, $h_3^* = 0.2$ W cm^{-2} K^{-1}.

Several simulations were performed in order to assess the effects of probe response on the thermodilution measurements. Examples of simulations are shown in figures 6 and 7. Both figures show a simulation of a step response, with the normalized temperature going from 0 to 1. In figure 6 the convection coefficient is 10 W cm^{-2} K^{-1} and in figure 7 the convection coefficient is 0.2 W cm^{-2} K^{-1}.

The result in figure 6 shows a situation where the probe response is limited by the probe body itself, since right in the beginning of the response, the response at the surface of the shell is brought to $T_\infty(t)$. Thus, the response is practically the same as if the temperature at the surface of the shell were kept at $T_\infty(t)$. In the result shown in figure 7, the response also depends on the convection coefficient.

2.2. Effects of probe response on the measurement of cardiac output

Over 100 simulations were performed in order to assess the effects of probe response on the estimate of cardiac output. In the first simulations, idealized thermodilution curves, such as the one illustrated as a full line in figure 1, were used as $T_\infty(t)$. Also, several convection coefficients (h) were used and, for each simulation, the convection coefficient was assumed to be constant. The results showed that the lower the value of h, the higher the degree of smearing of the curve. The fundamental question is whether or not the smearing of the curve changes the area under the curve. An extensive number of simulations with many different

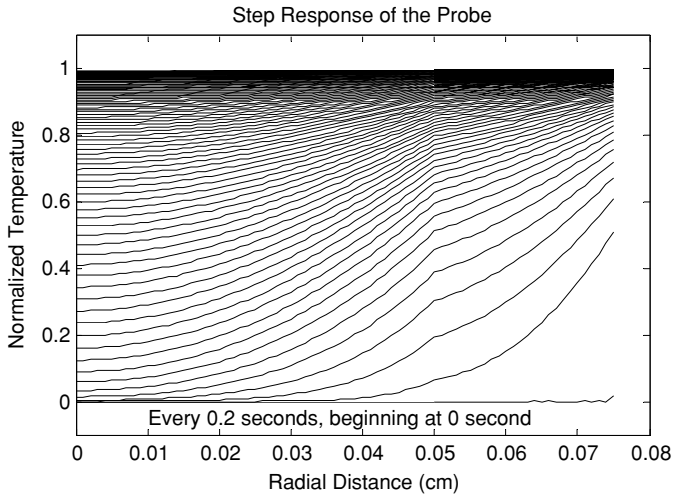

Figure 7. Step response of the thermistor sensor when the convection coefficient is 0.2 W cm^{-2} K^{-1}.

time-invariant values for h showed that in these cases the area does not change. This result is not surprising, as it can actually be predicted by looking at equation (23). In this equation, the measured value is equal to the convolution between $T_\infty(t)$ and the derivative of the step response. However, the area under the derivative of the step response is, by definition, equal to 1. Thus, there should be no change in area.

However, things get more complicated in a real thermodilution measurement situation where the convection coefficient is not constant. In the first 20% of the cardiac cycle (during the stroke), the convection coefficient is very high, and for the rest of the cycle it is very low as the flow velocity goes almost to zero. Because of this, the probe response is one during the stroke, but different during the remaining part of the cardiac cycle (evidence of this will be shown later on). Thus, the result when a constant convection coefficient is assumed may not always be valid.

Some simulations were performed using the equations of the proposed model, and these simulations showed clearly that, if the convection coefficient does not remain constant, the area of the smeared curve also changes.

Fortunately, for the specific kind of wave shape, with the specific flow profiles present in the thermodilution measurements, the area is preserved. The simulations showed that if the curve is composed of successive plateaux and the time behavior of the flow is the same for all plateaux, then the area under the curve is preserved.

In the simulations, the thermodilution curves were assumed to be idealized, like the solid line curve shown in figure 1, and the convection coefficient varied in several different ways during the plateau, but the variation pattern was the same for each plateau. For example, in one of the simplest simulations, a curve for a 60 bpm heart rate was generated assuming that during the first 0.2 s of the cardiac cycle the convection coefficient was 10 W cm^{-2} K^{-1}, and for the remaining 0.8 s this coefficient was 0.1 W cm^{-2} K^{-1}. Even though the simulation showed a remarkable amount of smearing, the area under the measured curve remained the same. The result of this simulation is shown in figure 8. The computed area under the smeared curve was 1.999 9997 (the area under the actual temperature is exactly 2.0). The very small error was due to computational rounding errors. A large number of other simulations with more

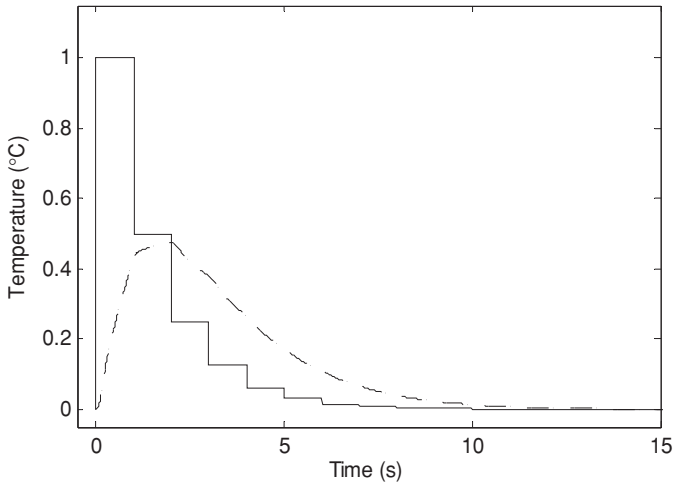

Figure 8. Simulation of the effect of the sensor response on an idealized thermodilution curve when the convection coefficient is not constant. Solid line: idealized thermodilution curve. Dashed line: smeared curve.

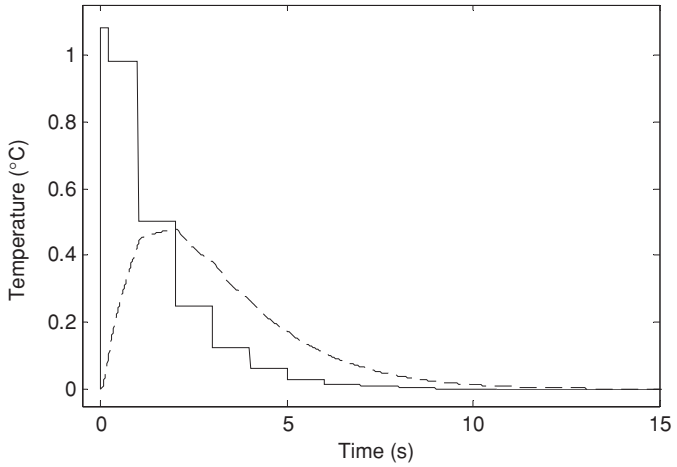

Figure 9. Simulation of the effect of the sensor response on an idealized thermodilution curve where the plateaux are not perfect. Solid line: idealized thermodilution curve. Dashed line: smeared curve.

complex profiles for the convection coefficient (but equal for all the plateaux) were performed, and the results always showed that the area under the curve is preserved.

Other simulations showed that if the true shape of $T_\infty(t)$ is not a perfect sequence of plateaux, or if the sequence of values for h were different for different plateaux, then there is an error associated with the measurement, and this error depends on how much the $T_\infty(t)$ curves deviate from a curve with perfect plateaux or on how much the flow velocity profiles change from plateau to plateau. As an example, one of the simplest performed simulations is illustrated in figure 9. In this simulation, the area under the curve was 2.016 (while the area under the original curve was 2.0). Thus, if the plateaux are not perfect, there are errors.

Extensive simulations showed that larger differences from the idealized curve lead to larger errors.

Other simulations dealt with a very common case where the response is not a perfect sequence of plateaux: the sinus arrhythmia. In this case, the R–R interval varies in a cyclic way around a mean value. As a result, the duration of the plateaux change in a cyclic way, and therefore the curve is not a perfect idealized curve. Several simulations were performed and, indeed, changes in the area under the curve were observed. These errors depend on the degree of arrhythmia. In a simulation with a fairly high degree of arrhythmia, an error of 1.9% was observed.

Another interesting conclusion drawn from the simulations is that the weighting factor used to describe the thermal to electrical conversion in the thermistor does not affect at all the area under the curve. In order to find this result, several simulations were performed and, for each simulation, the temperatures in 50 different positions in the thermistor body were calculated, and the integral of these temperatures was calculated. The results showed that, even though the curves are very different, the areas under them are exactly the same. Thus, if the average temperature is calculated over any region, the integral of this temperature curve will always be equal to the integral of the $T_\infty(t)$ curve. Thus, regardless of the weighting function, the area under the thermodilution curve will always be preserved for curves with the characteristics of the idealized thermodilution curve. A similar result was found by Valvano *et al* (1988).

In the next section, we present experiments to validate the model for the time response of the temperature sensor in thermodilution catheters.

3. Experimental validation of the theoretical model

In order to empirically characterize the time response of the Swan–Ganz thermistor, we applied a method in which a temperature sensor with very fast response (time to reach 63% of the maximum value in a plunge test in stirred water of 40 ms) is placed close to the slow sensor to be studied (time to reach 63% of the maximum value in a plunge test in stirred water of 1.7 s), and the temperature measured by the fast probe is assumed to be the true fluid temperature. The response of the slow probe (a Swan–Ganz thermistor) is obtained by comparing the two responses while we generate rapid perturbations in the temperature of the surrounding fluid. The two probes are placed in a flow at a reference temperature, and a temperature perturbation is generated by injecting the same fluid at a different temperature. In order not to disturb the flow too much, only a small amount of fluid at a higher or lower temperature is used. If the volume injected is kept low, the flow distortion should be negligible. For example, 3 ml was injected over a period of 0.2 s into a tube with a diameter of 1 cm with a flow of 0.2 m s^{-1}. The very small and quick change in speed is not important at all, because it is very small and the sensor is a few centimeters downstream the injection site, and the speed variation should disappear completely when the bolus reaches the probe site. The injection was very fast, in order to generate a high-speed temperature perturbation, resembling an impulse function with broad spectral band. Water was used in the tests, since its thermal properties are very close to those of blood.

Since the convection coefficient is kept constant in the experiments, the sensor response is linear and time invariant, and a technique based on the FFT is appropriate. To illustrate the technique, consider the measurements shown in the upper plot in figure 10, for the fast and slow probes in a 1 m s^{-1} flow. The sampling rate was 250 Hz. Theoretically, the areas under both curves should be equal. Temperature curves are normalized in the lower plot in figure 10 so that the summation of the amplitude of all samples is equal to 1.

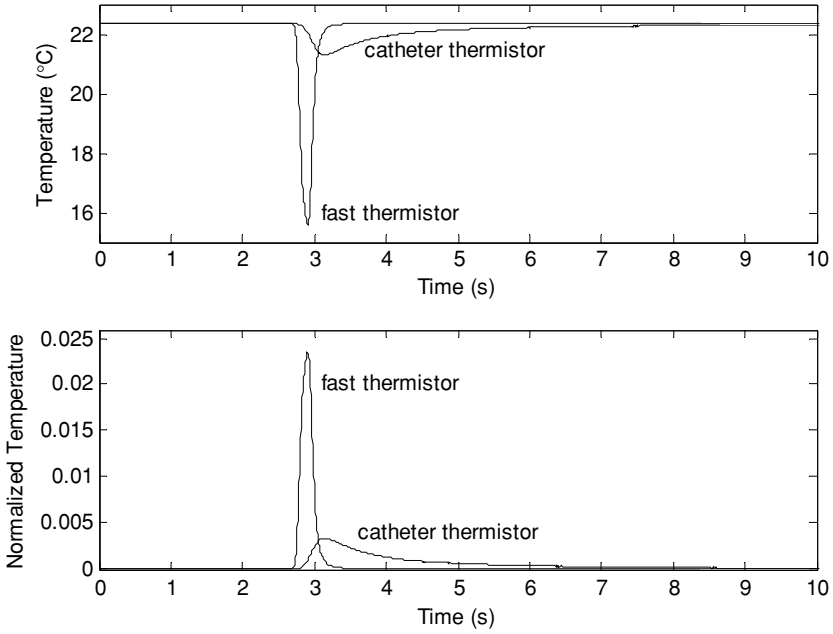

Figure 10. The responses of the fast and the Swan–Ganz thermistors. Upper plot: true temperature measurements. Lower plot: normalized temperatures.

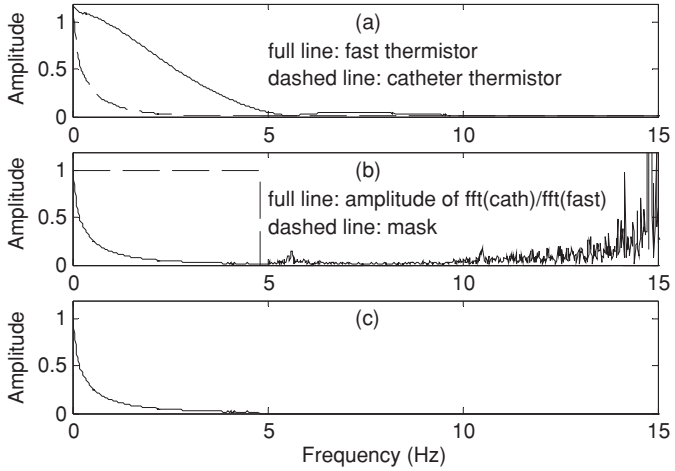

Figure 11. (a) The FFT of the signal measured by the Swan–Ganz (full line) and fast thermistors (dashed line). (b) Pointwise division of the FFTs of the Swan–Ganz and fast thermistor signals. (c) Frequency-limited estimate.

The Fourier transform of the normalized measurements is shown in figure 11(a). All the relevant frequencies are below 10 Hz and most of the information is concentrated below 5 Hz.

The technique to estimate the sensor response consists of calculating the FFTs of the slow and fast reference sensors and then dividing the former by the latter, thereby obtaining the transfer function $H(\mathrm{j}\omega)$ of the sensor. The transfer function is shown in figure 11(b).

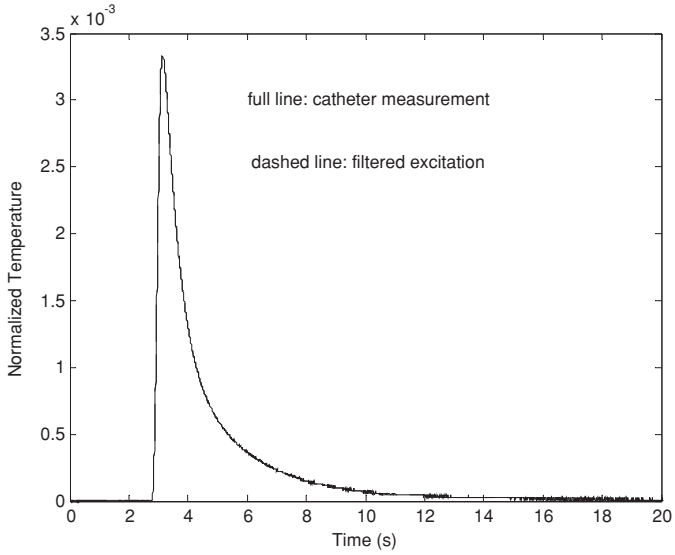

Figure 12. Plots of the temperature measured by the catheter and of the excitation temperature filtered by the estimated transfer function. Note that the curves are practically identical and it is practically impossible to distinguish them. This fact confirms the validity of the model.

The transfer function in figure 11(b) has significant noise at higher frequencies, because the signal magnitude at high frequencies is low, and the noise becomes comparable to the signal amplitude itself. Since all the relevant information is contained below 10 Hz, we can ignore higher frequencies. A simple simulation shows that the signal distortion is minimal even if we ignore frequencies above 5 Hz; accordingly, we set the transfer function to zero above 5 Hz (figure 11(c)).

To validate the estimate of the transfer function, we passed the input function (assumed to be equal to the measurement of the fast thermistor) through a filter whose transfer function in the frequency domain is shown in figure 11(c). Figure 12 shows that the temperature measured by the catheter sensor and the result of the filtered signal are in good agreement (the maximum observed error in the normalized temperature was 2.4×10^{-5}).

To obtain the impulse response of the probe, one can calculate the inverse FFT of the frequency response in figure 11(c). The impulse response is shown by the solid line in figure 13.

We showed that the impulse response of the temperature probes can be accurately expressed as a sum of exponentials. We used the method described by Lanczos (1988, chapter 4, on separation of exponentials), followed by an iterative best-fitting refinement. The estimate of the impulse response shown in figure 13 can be approximated by a summation of four exponential components:

$$h(t) = K(A\,\mathrm{e}^{-at} + B\,\mathrm{e}^{-bt} + C\,\mathrm{e}^{-ct} + D\,\mathrm{e}^{-dt}). \tag{24}$$

The approximation is shown as a dotted line in figure 13, with the parameter values of A, a, B, b, C, c, D and d shown in the figure. The multiplier of the first exponential (A) is normalized to 1, and K is chosen so that the summation of all samples in the digitized impulse response is 1. The four-exponential approximation is reasonably close to the estimate (the average absolute error in the normalized temperature is 5.2×10^{-6} and the maximum error was 4.7×10^{-4}). An approximation with three exponentials was examined and had a

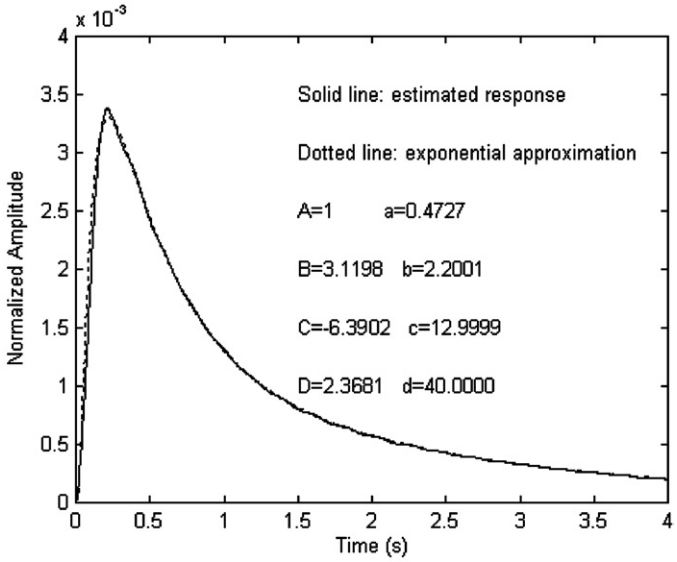

Figure 13. An estimate of the step response of the catheter probe (solid line) and an approximation by a summation of four exponential components (dotted line). Note that the curves are practically identical and it is practically impossible to distinguish them.

somewhat higher error (the average absolute error in the normalized temperature is 6.8×10^{-6} and the maximum error was 9.5×10^{-4}) than the approximation with four exponentials (a 1.3 times larger average absolute error and a two times larger maximum error, but only at the peak of the response). To show that the approximation is sufficiently accurate, a simulation was run in which the same stimulus is passed through the low-pass filter represented by the four-exponential transfer function. The result, presented in figure 14, shows a very small error for this stimulus. Even smaller errors can be expected for stimuli with lower frequency content.

The experiments above were performed in constant flow (1 m s^{-1}). The results show that the probe response can be written as a convolution operation between the bulk temperature of the surrounding fluid and the impulse response of the probe. However, this result is only valid for a time-invariant distribution of h surrounding the sensor. Unfortunately, the flow in the pulmonary artery is not constant, but pulsatile. In order to assess the effect of the variation of the flow in the pulmonary artery, we performed similar experiments with a number of flow rates. Figure 15 shows the estimated responses and illustrates how the response of a thermodilution catheter is dependent on the fluid speed or, equivalently, on the convection coefficient h.

In figure 15, the curves for flow velocities of 1.0, 0.8 and 0.6 m s^{-1} were very close. The curve for 0.4 m s^{-1} was a little more smeared, but still close to the first three, and the curve for 0.2 m s^{-1} was the most smeared of all, but it was still very close to the other ones. It is noticeable that even for the lower flows, the response is still close to the response at high flows. This happens because the thermal conductivity of the epoxy protection is low compared to the convective component of the moving blood, and the convection component is strong enough to keep the probe surface close to the fluid temperature. Therefore, the response of this particular probe does not depend much on the flow if the flow velocities are within the range studied.

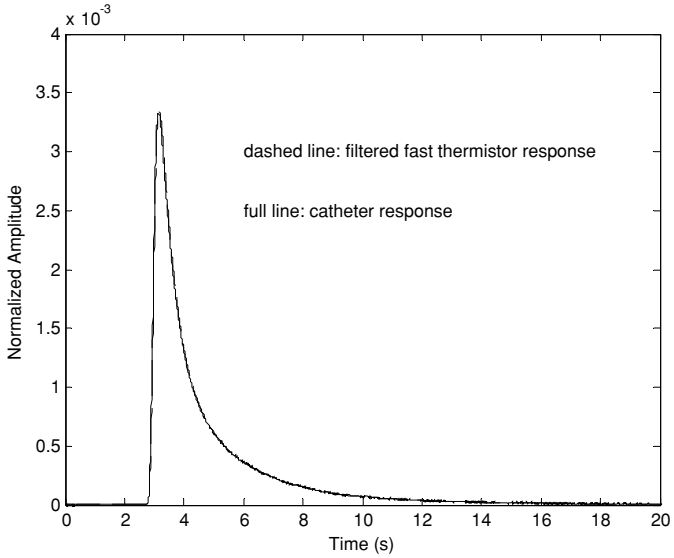

Figure 14. The catheter response to the stimulus in figure 10 and the signal filtered by the low-pass filter represented by the four-exponential kernel. Note that the curves have very similar behavior.

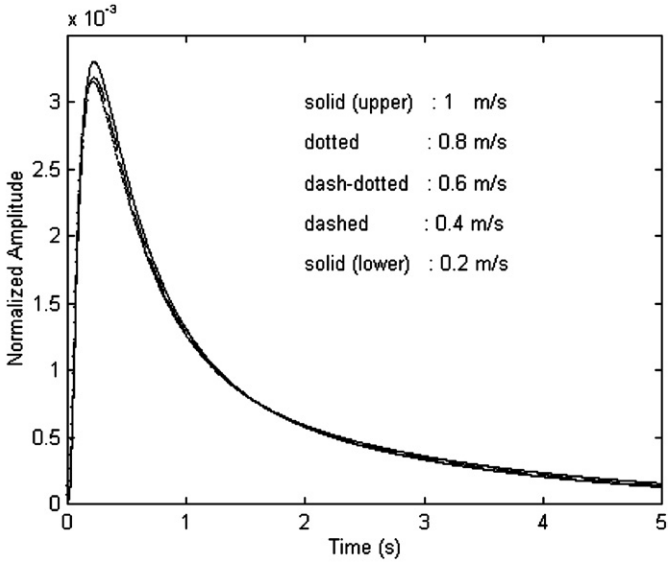

Figure 15. Estimate of the probe impulse responses for five different flows. Note that the curves are practically identical.

This last result shows that this probe can be used to measure temperatures in media with time-varying velocities within the range of the flows that were used in this experiment and, that within this range, the probe will behave like a linear time-invariant system.

One missing piece of information is characterization of the probe response in flows with velocities below 0.2 m s^{-1}. At some point below this speed, the probe will likely have a slower time response, up to a limit where it will behave approximately like a probe embedded in a

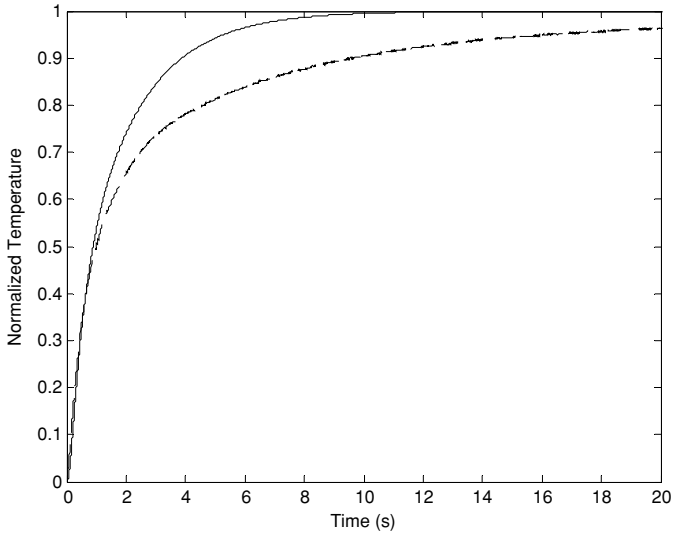

Figure 16. Estimates of the step response of the probe for speeds higher than 0.2 m s^{-1} (solid line) and at 0 m s^{-1}.

solid. Even though due to technical limitations we did not characterize the probe for flow velocities from 0 to 0.2 m s^{-1}, we did get an estimate of the impulse response for the lower limit case (velocity equal to 0 m s^{-1}). In order to obtain this estimate, we performed a plunge test in still water. To show that the response is different for a flow of 0 m s^{-1} and flows above 0.2 m s^{-1}, we obtained the step response by integrating the impulse response for the flow with velocity above 0.2 ms and plotted together the two estimates of the step response in figure 16.

This last result shows that the probe response indeed changes for lower speeds, and further studies evaluating probe behavior in this range are required.

4. Discussion

The theoretical model for the behavior of the temperature sensor of the Swan–Ganz catheter demonstrates that the time response of this sensor is composed of an infinite number of exponential components, and the experimental results showed that only a few (three or four) components provide an excellent approximation. The model also demonstrated that, for constant flows or time-variant flows with high speed, the system is linear and time invariant, and that the probe response can be written as a convolution operation between the bulk temperature of the surrounding medium and the derivative of the probe's step response. This result is important if one wishes to use deconvolution approaches in order to enhance thermodilution curves (Santos *et al* 2002).

The proposed empirical method for probe response estimation should work in general, and it is a good choice whenever a good estimate of the excitation signal is available, usually by using a very fast sensor. A spikelike excitation, such as the one shown in figure 8, is very convenient because it contains components with a large range of frequencies, allowing a better estimate at higher frequencies. In addition, this kind of function has zeros only above the relevant frequencies of the signal. If the spectrum of the excitation function has zeros in meaningful frequencies, special techniques for recovery of the information in the frequencies

containing zeros have to be applied (Arsenault and Genestar 1971, Bernier and Arsenault 1991).

Simulations were performed, which made clear that four exponential components provide an extremely precise approximation, three components provide a precise approximation, two components provide a good approximation and one exponential provides only a rough estimation. If one does the fitting procedure with one exponential, one could get a rough but qualitatively meaningful description of the probe behavior, but with two or more exponentials the description would be much more accurate.

These results are significant, as they shed some light on the behavior of the temperature sensors embedded in thermodilution catheters. However, they do not settle the problem completely. It was shown that, for the range of fluid speeds from 0.2 to 1 m s^{-1}, the probe response is practically the same. Flows in the pulmonary artery can be close to zero. Therefore, it is clear that it is still necessary to develop another detailed model for the stage where the flow is very small, and further studies on how these models reflect in the global behavior of the probe through the whole cardiac cycle are required. Even though the need for an accurate model for the probe behavior in still liquid is evident, the results presented in section 2 showed that the lack of knowledge regarding the probe behavior during the period following the stroke causes negligible inaccuracies in cardiac output measurements, as long as the true behavior of the bulk blood temperature at the pulmonary artery remains close to the behavior of an idealized thermodilution curve where the temperature plateaux are perfectly flat.

5. Conclusion

The results of this work showed that, if the blood flow is higher than 0.2 m s^{-1}, the response of the thermodilution catheter is linear and time invariant even if the flow velocity varies within this range, and that at lower flows, the response is still linear and time invariant but only if the convection coefficient does not vary with time. In the case of thermodilution, experiments showed that the probe response is one within the ejection period but different in the remaining period of the cardiac cycle. The simulation results showed that if the convection coefficient changes with time, then in general the area under the thermodilution curve is not preserved, and that this could be a source of error in the thermodilution method. However, the results also showed that, for the very specific shape of the idealized thermodilution curve where the curve is formed by successive plateaux and the time behavior of the flow for each plateau is the same, the area under the curve is indeed preserved and there is no error. We further showed that if the actual thermodilution curve is very different from the idealized thermodilution curve, small errors can result. Simulations showed errors of 1.9% measured during a fairly high degree of sinus arrhythmia.

Acknowledgments

The present work was accomplished with the support of K Takaoka, CNPq and CAPES.

References

Arsenault H and Genestar B 1971 Deconvolution of experimental data *Can. J. Phys.* **49** 1865–8

Bernier R and Arsenault H H 1991 Deconvolution of two-dimensional images with zeros in the transfer function *Appl. Opt.* **30** 5163–8

Bloomfield D A 1973 *Dye Curves: The Theory and Practice of Indicator Dilution* (Baltimore, MD: University Park Press)

Dow P 1956 Estimations of cardiac output and central blood volume by dye dilution *Physiol. Rev.* **36** 77–102

Fegler G 1954 Measurement of cardiac output in anaesthetized animals by a thermodilution method *Q. J. Exp. Physiol. Cogn. Med. Sci.* **39** 153–64

Fegler G 1957 The reliability of the thermodilution method for determination of the cardiac output and the blood flow in central veins *Q. J. Exp. Physiol. Cogn. Med. Sci.* **42** 254–66

Ganz W and Swan H J 1972 Measurement of blood flow by thermodilution *Am. J. Cardiol.* **29** 241–6

Lanczos C 1988 *Applied Analysis* (New York: Dover)

Marushak G F and Schauble J F 1985 Limitations of thermodilution ejection fraction: degradation of frequency response by catheter mounting of fast-response thermistors *Crit. Care Med.* **13** 679–82

Mikhailov M D and Ozisik M N 1984 *Unified Analysis and Solutions of Heat and Mass Diffusion* (New York: Wiley)

Ozisik M N 1993 *Heat Conduction* 2nd edn (New York: Wiley)

Rocha A F 1997 The dynamic behavior of thermistor probes *PhD Dissertation* The University of Texas at Austin

Santos I, Rocha A F, Nascimento F A O and Valvano J W 2002 Measurement of ejection fraction with standard thermodilution catheters *Med. Eng. Phys.* **24** 325–35

Swan H J C, Ganz W, Forrester J, Marcus H, Diamond G and Chonette D 1970 Catheterization of the heart with the use of a flow-directed balloon-tipped catheter *N. Engl. J. Med.* **283** 447–51

Taylor B C and Sheffer D B 1990 Understanding techniques for measuring cardiac output *Biomed. Instrum. Technol.* **24** 188–97

Trautman E D and Newbower R S 1984 The development of indicator-dilution techniques *IEEE Trans. Biomed. Eng.* **31** 800–7

Trautman E D and Newbower R S 1988 Thermodilution measurement of cardiac output *Encyclopedia of Medical Devices and Instrumentation* ed J G Webster (New York: Wiley)

Valvano J W, Anderson G, Pearce J, Hayes L and White C A 1988 Coupled electrical and thermal finite element model of self-heated thermistors *World Congress on Medical Physics and Biomedical Engineering (San Antonio, Texas)*

von Reith E A and Versprille A 1988 Indicator dilution measurement of cardiac output *Encyclopedia of Medical Devices and Instrumentation* ed J G Webster (New York: Wiley)

Webster J G 1998 Measurement of flow and volume of blood *Medical Instrumentation: Application and Design* ed J G Webster (Boston, MA: Houghton Mifflin)